Geochimica et Cosmochimica Acta, Vol. 69, No. 13, pp. 3419–3430, 2005

0016-7037/05 $30.00 + .00

doi:10.1016/j.gca.2004.11.001

Carbon-rich chondritic clast PV1 from the Plainview H-chondrite regolith breccia: Formation from H3 chondrite material by possible cometary impact

Alan E. Rubin,[1,*] Josep M. Trigo-Rodriguez,[1] Takuya Kunihiro,[1] Gregory W. Kallemeyn,[1] and John T. Wasson[1,2,3]

[1]Institute of Geophysics and Planetary Physics,
[2]Department of Earth and Space Sciences, and
[3]Department of Chemistry and Biochemistry, University of California, Los Angeles, CA 90095-1567, USA

(*Received April* 29, 2004; *accepted in revised form November* 2, 2004)

Abstract—Chondritic clast PV1 from the Plainview H-chondrite regolith breccia is a subrounded, 5-mm-diameter unequilibrated chondritic fragment that contains 13 wt% C occurring mainly within irregularly shaped 30–400-μm-size opaque patches. The clast formed from H3 chondrite material as indicated by the mean apparent chondrule diameter (310 μm vs. ~300 μm in H3 chondrites), the mean Mg-normalized refractory lithophile abundance ratio (1.00 ± 0.09×H), the previously determined O-isotopic composition ($\Delta^{17}O$ = 0.66‰ vs. 0.68 ± 0.04‰ in H3 chondrites and 0.73 ± 0.09‰ in H4-6 chondrites), the heterogeneous olivine compositions in grain cores (with a minimum range of Fa1-19), and the presence of glass in some chondrules. Although the clast lacks the fine-grained, ferroan silicate matrix material present in type 3 ordinary chondrites, PV1 contains objects that appear to be recrystallized clumps of matrix material. Similarly, the apparent dearth of radial pyroxene and cryptocrystalline chondrules in PV1 is accounted for by the presence of some recrystallized fragments of these chondrule textural types. All of the chondrules in PV1 are interfused indicating that temperatures must have briefly reached ~1100°C (the approximate solidus temperature of H-chondrite silicate). The most likely source of this heating was by an impact. Some metal was lost during impact heating as indicated by the moderately low abundance of metallic Fe-Ni in PV1 (~14 wt%) compared to that in mean H chondrites (~18 wt%). The carbon enrichment of the clast may have resulted from a second impact event, one involving a cometary projectile, possibly a Jupiter-family comet. As the clast cooled, it experienced hydrothermal alteration at low water/rock ratios as evidenced by the thick rims of ferroan olivine around low-FeO olivine cores. The C-rich chondritic clast was later incorporated into the H-chondrite parent-body regolith and extensively fractured and faulted. *Copyright © 2005 Elsevier Ltd*

1. INTRODUCTION

Carbon is a minor component of chondritic meteorites: type 3 ordinary chondrite (OC) falls typically contain 0.3–0.6 wt% C, two CV3 falls (Allende and Bali) also contain 0.3–0.6 wt% C, CM2 falls contain ~1.8 wt% C, and CI Orgueil contains 2.8 wt% C (Jarosewich, 1990). Poorly graphitized carbon occurs within metallic Fe-Ni grains and as relatively abundant sub-millimeter-size carbon-rich aggregates in some type 3 OC (McKinley et al., 1981; Scott et al., 1981a; Brearley, 1990; Mostefaoui et al., 2000). Far more C (6–13 wt%) is present in four enigmatic chondritic clasts described by Scott et al. (1981a,b). The clasts range in diameter from 1 to 11 mm and occur in H-chondrite regolith breccias: PV1 from Plainview (1917) (hereafter Plainview), DT1 and DT2 from Dimmitt, and WN1 from Weston. The clasts have also been reported to lack the fine-grained ferroan-silicate-rich matrix material (Scott et al., 1981a,b, 1988; Brearley, 1990) that occurs ubiquitously in type 3 ordinary (Huss et al., 1981) and carbonaceous (McSween and Richardson, 1977) chondrites.

Previous studies have concluded that the C-rich chondritic clasts formed in the solar nebula and are thus most likely composed of primitive material (Scott et al., 1981b, 1988; Brearley, 1990). In contrast, the present study of the PV1 chondritic clast indicates that most features were produced by asteroidal processes.

* Author to whom correspondence should be addressed (aerubin@ucla.edu).

2. ANALYTICAL PROCEDURES

A significant fraction of clast PV1 occurs within University-of-New-Mexico thin section UNM 273 of the Plainview H-chondrite regolith breccia (Fig. 1a). We studied this thin section microscopically in transmitted and reflected light and prepared a mosaic back-scattered electron (BSE) image of the clast. A grid was superimposed on this image; labels of chondrules and other objects in the image reflect their location on this grid. All BSE images were made with the LEO 1430 VP scanning electron microscope (SEM) at UCLA using a 15 keV acceleration voltage and a working distance of ~19 mm. Chondrule and grain sizes were measured on the BSE images. Mineral compositions were determined with the JEOL JXA-8200 electron microprobe at UCLA using natural and synthetic standards, an accelerating voltage of 15 keV, a 15-nA sample current, 20-s counting times, and ZAF corrections.

A 5.46-mg chip of PV1, obtained from the University of New Mexico, was separated for instrumental neutron activation analysis (INAA). The sample was irradiated at the University of California, Irvine (UCI) reactor with a neutron flux of $\sim 1.8 \times 10^{12}$ cm^{-2} s^{-1}. Samples were irradiated for two minutes and then counted immediately to determine elements producing very short-lived radioisotopes (Mg, Al, Ca, V and Mn). Samples were irradiated again for 4 h and counted several times over a period of ~6 weeks to determine elements producing longer-lived species (Na, K, Ca, Sc, Cr, Mn, Fe, Co, Ni, Zn, Ga, As, Se, La, Sm, Eu, Tb, Ho, Yb, Lu, Ir and Au). The INAA procedure is described in Kallemeyn et al. (1989). The estimated relative sample standard deviations are 6%–10% for K, Eu, Yb and Lu, and ≤5% for all other elements.

3. RESULTS

3.1. Petrography and Mineralogy

3.1.1. Plainview whole rock

Plainview is an H-chondrite regolith breccia (fig. 1 of Fodor and Keil, 1976) containing solar-wind-implanted rare gases (Schultz

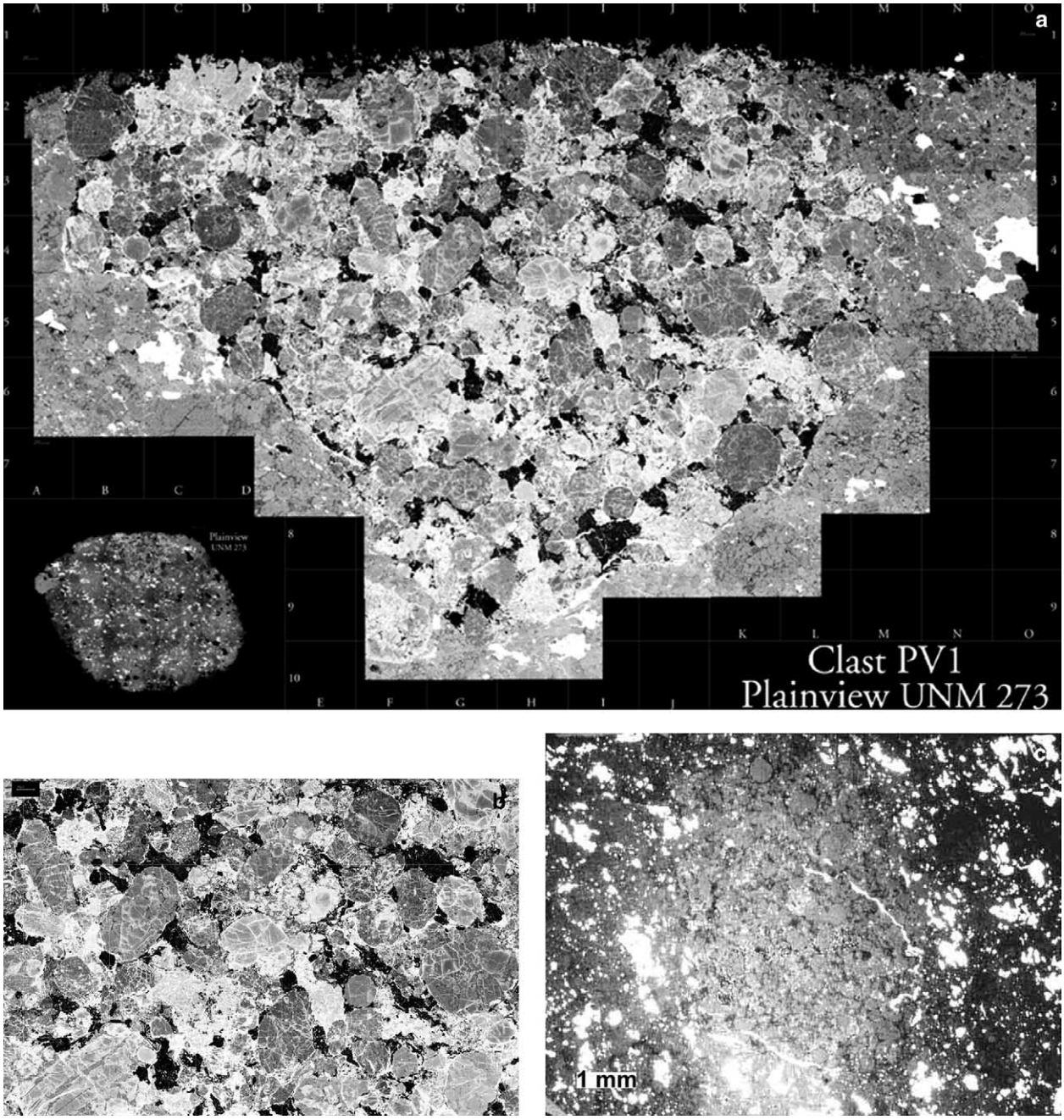

Fig. 1. Clast PV1. (a) Back-scattered electron (BSE) image of the PV1 clast and the surrounding Plainview host. The grid used in locating and identifying components is superposed on the image. The location of the clast relative to the entire thin section is shown at lower left. (b) Portion of a mosaic of the BSE image of PV1 within the Plainview host. The clast contains abundant C-rich aggregates (black) and fused chondrules (shades of gray) of different textural types and compositions. Small scale bar at upper left is 100 μm long. (c) Reflected light image of PV1 showing prominent veins of metallic Fe-Ni (white) penetrating the clast from the Plainview host.

and Kruse, 1989). The meteorite was found in Hale County, Texas; ~700 kg have been recovered (Grady, 2000). Plainview contains ~30 vol% H5 clasts, ~1 vol% light-colored impact-melt-rock clasts, ≤1 vol% exotic clasts (mainly phyllosilicate-bearing CM2 chondrite fragments), and <1 vol% shocked (but unmelted) H-chondrite clasts of different petrologic types (Fodor and Keil, 1976; Rubin, 1982); the remaining ~70 vol% consists of clastic chondritic material surrounding recognizable clasts.

The Plainview whole rock comprises subrounded ~0.02–40-mm-size clasts surrounded by glassy-to-microcrystalline feldspathic material (Bischoff et al., 1983). Plainview was classified as shock-stage S3, indicating that the examined portions of the breccia experienced a peak shock pressure of 5–10 GPa (Stöffler et al., 1991). Plainview contains opaque shock veins, melt pockets and weakly developed melt dikes (Stöffler et al., 1991).

The numerous impact-melt-rock clasts in Plainview are generally very similar in bulk composition to the silicate portion of the Plainview host, consistent with the view that they formed from the host by impact melting, separation of a dense, immiscible metal-sulfide liquid from the silicate liquid, and rapid cooling of the residual silicate melt (Fodor and Keil, 1976). The ^{39}Ar-^{40}Ar age of one 1.5 × 4-cm-size impact-melt-rock clast is 3.63 Ga; the age of the Plainview host is 4.4 Ga (Keil et al., 1980).

3.1.2. Clast PV1

PV1 is a subrounded 5-mm-diameter dark-colored chondritic clast (Fig. 1a,b) that contains ~13 wt% carbonaceous matter (predominantly poorly graphitized C) occurring mainly within irregularly shaped 30–400-μm-size opaque patches (Fodor and Keil, 1976; Scott et al., 1981a,b, 1988; Brearley, 1990; this study). Modal analysis indicates that the clast contains ~6 vol% (i.e., ~14 wt%) metallic Fe-Ni (Scott et al., 1981b); however, this is an upper limit because some of the metal occurs in veins (particularly two prominent subparallel 2–2.5-mm-long veins; Fig. 1c) that are not indigenous to the clast (Scott et al., 1981b; this study).

3.1.2.1. Mineral compositions. Olivine and low-Ca pyroxene are compositionally heterogeneous: mean Fa = 17 ± 8 mol% (PMD = 46); mean Fs = 10.6 ± 6.3 mol% (PMD = 48) (Scott et al., 1981b). These compositional distributions (Fig. 2) roughly resemble those of moderately primitive (type ~3.6) OC (e.g., fig. 1 of Dodd et al., 1967). The paucity of Fa 0–2 grains in the PV1 olivine distribution is most similar to that of H/L3.6 Tieschitz (fig. 1 of Dodd et al., 1967).

3.1.2.2. Chondrules. Chondrules, chondrule fragments and coarse silicate grains together constitute 63 vol% of PV1 (Scott et al., 1981b). Most chondrules are type I and type II porphyritic olivine (PO) and porphyritic olivine-pyroxene (POP). Two barred olivine (BO) chondrules (e.g., Fig. 3a) and a few small granular olivine-pyroxene (GOP) chondrules occur in the thin section we studied. Very rare enveloping compound chondrules and radial pyroxene (RP) chondrules are also present. No readily recognizable cryptocrystalline chondrules were encountered. Glassy mesostasis occurs between the bars in the two BO chondrules (e.g., Fig. 3a) as well as between phenocrysts in some PO and POP chondrules. We measured the apparent diameters of 60 chondrules in PV1 and found a mean apparent diameter of 310 ± 120 μm.

3.1.2.3. Fractures. Numerous 1–3-μm-thick, 20–160-μm-long, cross-cutting fractures transect every chondrule in the PV1 clast (e.g., Fig. 3b). The fractures appear bright in BSE images, reflecting the fact that they are filled with thin veins of opaque material: some veins contain troilite, some contain goethite, and some contain both phases. (Goethite is a terrestrial weathering product.) In a few cases, troilite and goethite occur together as adjacent parallel veins filling the same fracture.

3.1.2.4. Chondrule fusion. Most interfaces between adjacent chondrules are melded together (Fig. 4). The boundaries between many chondrules are identifiable only because of the change in texture and grain size between adjacent chondrules of distinct textural types. Mineral grains at the interfaces between different chondrules abut each other, in most cases with no discernable gap. Although some chondrules are partly surrounded by C-rich patches, other parts of the perimeters of these chondrules are finely intergrown with those of adjacent chondrules. The chondrule boundaries resemble those of compound chondrules (figs. 1–3 of Wasson et al., 1995) that fused in the nebula.

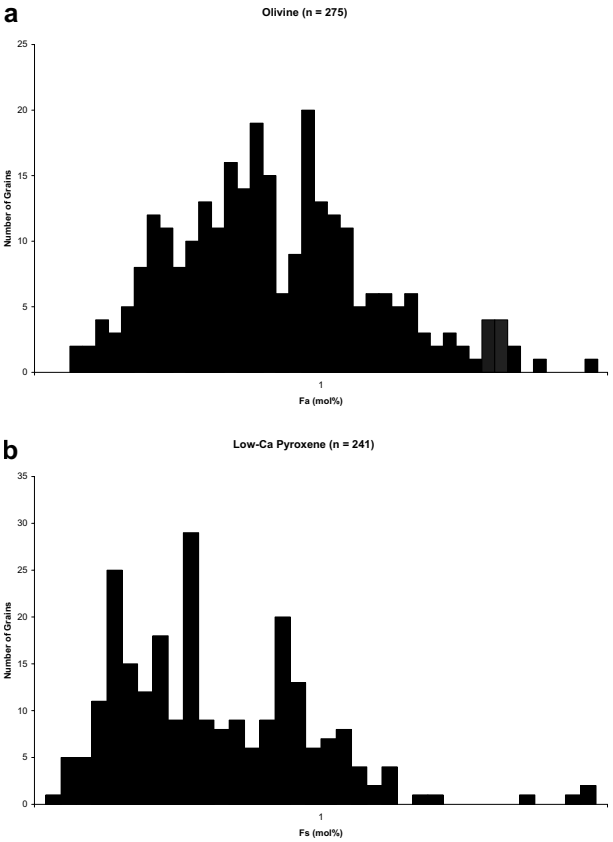

Fig. 2. Compositional distributions of mafic minerals in clast PV1 determined by random electron microprobe analysis of ~>5-μm-size grains. (a) Olivine (n = 275 grains) is very heterogeneous, but there is a paucity of grains at very low Fa contents. The relative dearth of grains at Fa19-20 is probably an artifact. (b) Low-Ca pyroxene (n = 241 grains) is also very heterogeneous, but there is a paucity of grains at low Fs contents. As in typical highly unequilibrated type 3 OC, the mean Fs content has a lower numerical value than the mean Fa content. Data from Scott et al. (1981b).

3.1.2.5. Recrystallized nonporphyritic chondrules. Although few RP chondrules and no cryptocrystalline chondrules were identified in the available thin section of PV1, there are objects that appear to be recrystallized fragments of these textural types. For example, chondrule E6 (Fig. 5a) is a distorted-oval-shaped 230 × 370-μm-size object that consists of at least two distinct sets of subparallel irregular bars of low-Ca pyroxene (Fs16.7Wo3.3); the bars range in length from ~70–120 μm and in thickness from 1.8–4 μm. Small (1–4-μm-thick) patches of interstitial glass occur between the bars. The

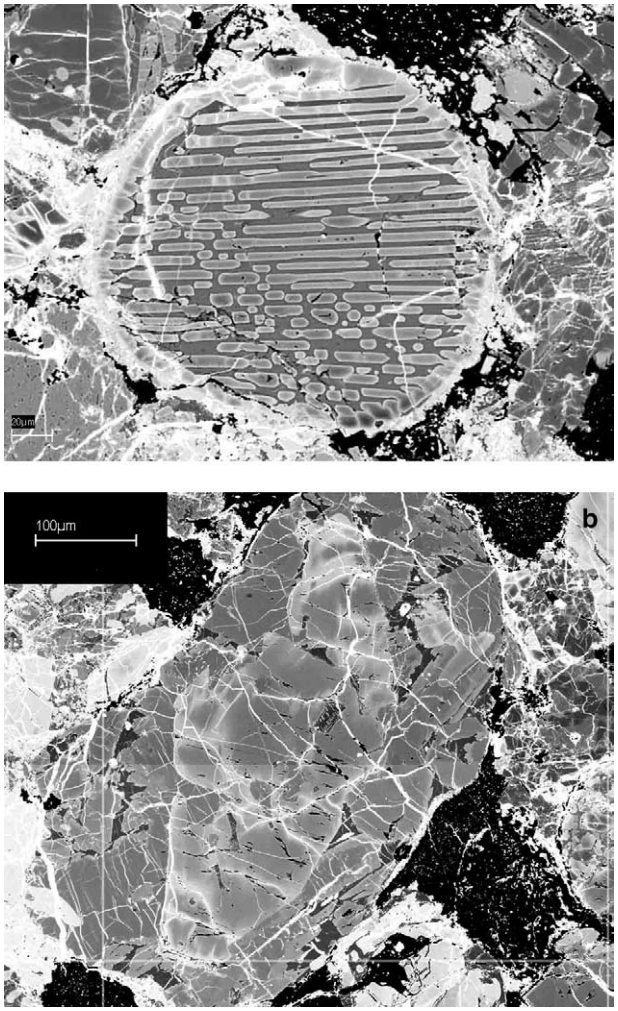

Fig. 3. Chondrules. (a) Rimmed barred olivine (BO) chondrule B4 containing abundant glassy mesostasis between the olivine bars. Several bars and grains near the rim have low-FeO cores surrounded by high-FeO olivine. A few fractures (white) transect the chondrule. Scale bar at lower left is 20 μm in length. (b) Porphyritic olivine (PO) chondrule G4 transected by numerous fractures (white) filled with goethite and/or troilite. Both images in BSE.

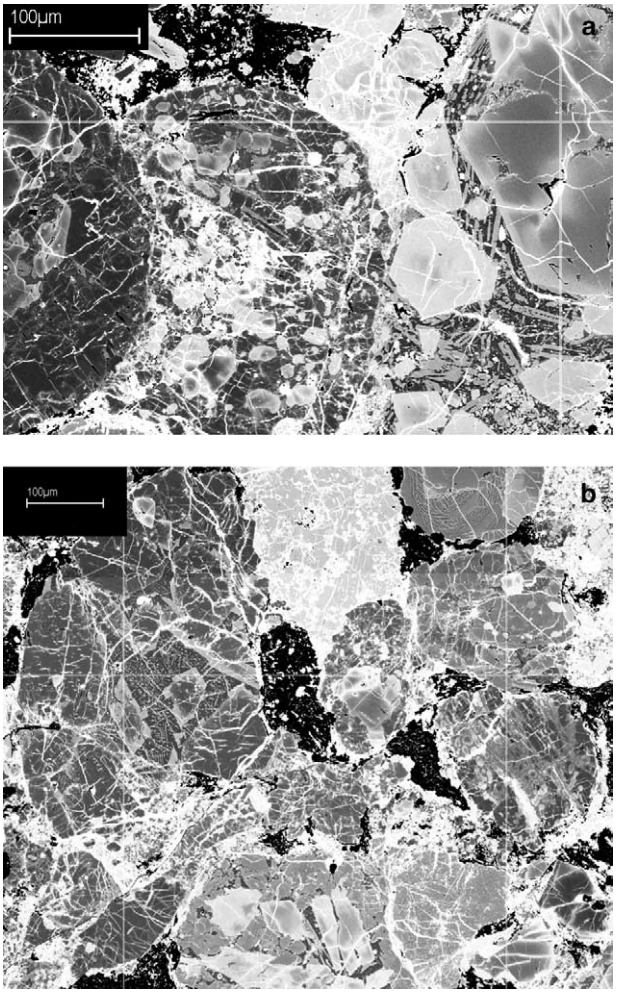

Fig. 4. Fused chondrules. (a) Region D4 consisting of intergrown porphyritic chondrules of different compositions and grain sizes. (b) Region I5 consisting of intergrown porphyritic chondrules interspersed with small C-rich aggregates (black).

sets of bars are inclined with respect to each other at an angle of ~40°. A few 4–20-μm-size anhedral and subhedral low-Ca pyroxene grains are present between some of the bars. E6 is inferred to be a recrystallized RP chondrule.

Chondrule D2 (Fig. 5b) appears to be a recrystallized cryptocrystalline chondrule fragment. It is 720 μm in diameter and consists of 2–3-μm-size grains of low-Ca pyroxene (Fs38.8Wo1.4) and rare subcalcic augite (Fs23.1Wo23.1) separated by ~1-μm-size voids. In many places, the small pyroxene grains appear to be aligned to form ~100-μm-long, 2–3-μm-thick pyroxene bars. In different regions the bars are oriented in different directions. Thin troilite veins (typically 1 × 10 μm) occur between some of the bars. Numerous fractures filled with goethite transect the chondrule.

3.1.2.6. Recrystallized fine-grained silicate matrix material. Although patches of fine-grained, FeO-rich, interchondrule silicate matrix material are ubiquitous in type 3 OC (Huss et al., 1981), this material appears to be absent from PV1 (as well as the other C-rich chondritic clasts) (Scott et al., 1981a,b). There are, however, a few objects in PV1 that appear to be recrystallized clumps of matrix material. One such object (I5; Fig. 5c) consists of ~20 vol% small (1–17 μm), moderately angular taenite and troilite grains, ~30 vol% pore space presently filled with C-rich material, and ~50 vol% small (0.5–3 μm) silicate grains. The silicates are mainly ferroan olivine (Fa36.0) with minor subcalcic augite (Fs18.4Wo25.2). Rare grains of low-Ca pyroxene (Fs12.4Wo0.28) are also present. Several fractures transect the object.

3.1.2.7. Ferroan olivine in chondrules. Many porphyritic chondrules, porphyritic chondrule fragments and isolated olivine grains in PV1 possess slightly fractured relict cores of low-FeO olivine surrounded by moderately fractured ferroan olivine patches (Fig. 6). In many cases, ferroan olivine halos surround fractures in low-FeO olivine cores in the chondrules. For example, object C4 (Fig. 6a) is a 175 × 215-μm-size POP

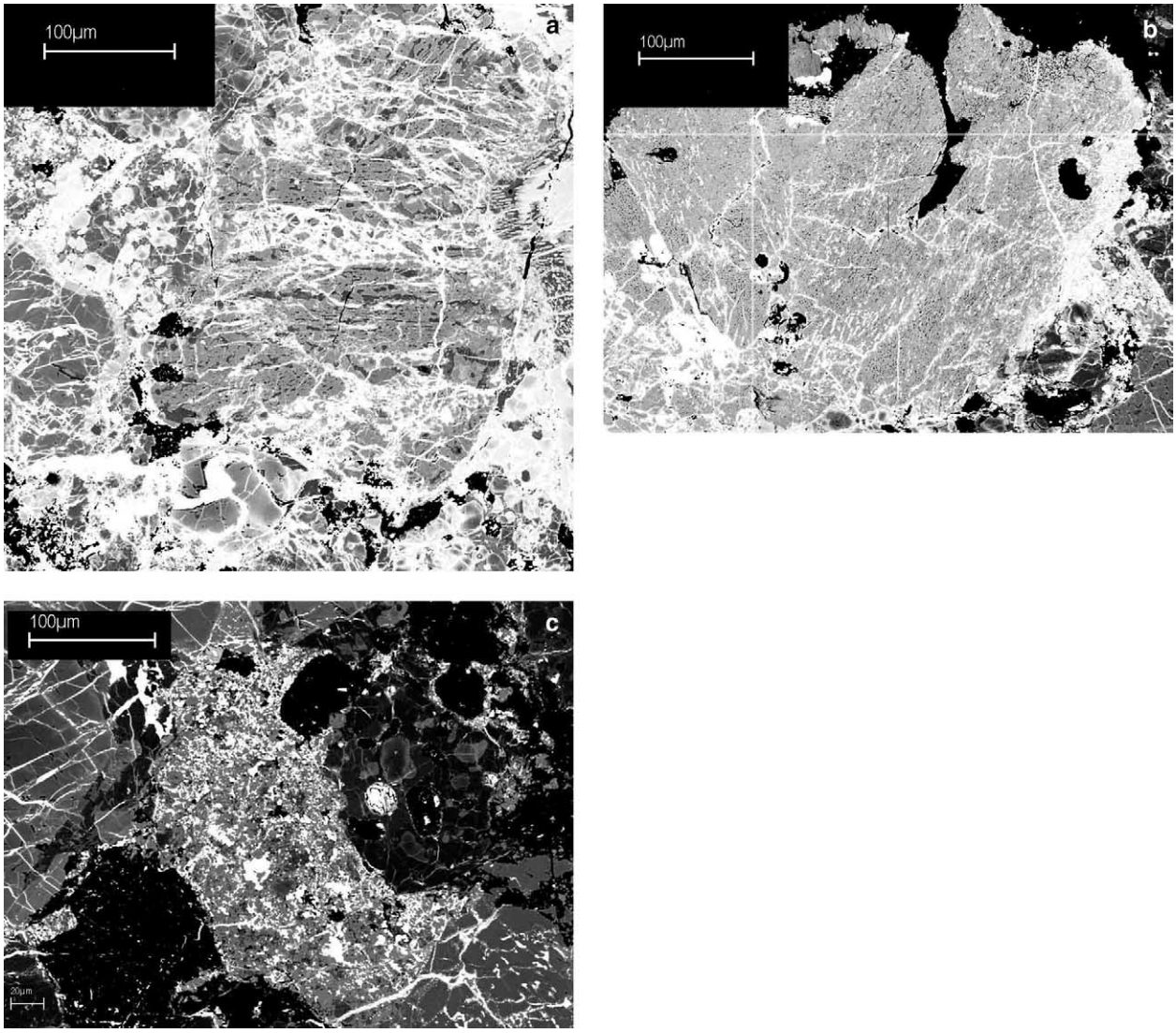

Fig. 5. Recrystallized chondrules and fine-grained matrix. (a) Partly recrystallized radial pyroxene (RP) chondrule E6 containing at least two sets of distorted pyroxene bars and interstitial glass. Numerous fractures transect the chondrule. (b) Recrystallized cryptocrystalline chondrule D2 consisting of small pyroxene grains separated by small voids (that are at present filled with C-rich aggregate material). (c) Recrystallized clump of fine-grained silicate matrix material I5 containing numerous grains of metallic Fe-Ni and sulfide (white); most of the silicate (dark gray) consists of ferroan olivine.

chondrule fragment containing 6 × 9–75 × 115-μm-size ferroan olivine grains (Fa32.7–35.7), 20–30-μm-size grains of low-Ca pyroxene (Fs15.1Wo4.3) and pigeonite (Fs15.0Wo8.9), and interstitial mesostasis. The largest olivine grain consists of several 5–18-μm-size relict relatively low-FeO (Fa12.0) cores surrounded by thick patches (up to 45 μm thick) of ferroan olivine (Fa35.7). The outer portion of the grain is composed entirely of ferroan olivine; 2–3-μm-thick bands of ferroan olivine also surround the troilite veins that fill the fractures.

Object D3 (Fig. 6b) is a wedge-shaped PO chondrule fragment, 220 × 360 μm in size. It contains coarse (40 × 60–105 × 205 μm) olivine grains consisting of ~20 vol% small (7 × 11–25 × 35 μm) relatively low-FeO patches (Fa19.4) surrounded by ferroan olivine (~80 vol%; Fa32.5). The outer parts of the grains consist entirely of ferroan olivine.

Object K3 is a 290 × 300-μm-size isolated olivine grain consisting of relict relatively low-FeO (Fa13.5) zones ranging in size from 10 × 10 μm to 50 × 110 μm, hemmed in by fractures filled with troilite veins and surrounded by ferroan olivine (Fa30.1) zones up to 80 × 105 μm in size. Thin (2–10-μm-thick) patches of ferroan olivine surround most of the troilite veins.

Enveloping compound-chondrule G7 (Fig. 6c) consists of a 200-μm-diameter recrystallized RP core (with Fs7.1Wo1.7 low-Ca pyroxene grains) surrounded by a ~140-μm-thick spherical shell consisting mainly of small (3–9-μm-size) euhedral olivine grains surrounded by mesostasis. Many of these grains have 3–5-μm-size low-FeO relict cores (Fa9.4–13.8) surrounded by 1–1.5-μm-thick ferroan olivine rims (Fa23.6–29.0) (Fig. 6d). Many of the euhedral olivine grains are transected by 0.7-μm-wide fractures filled with ferroan olivine.

Barred olivine chondrule B4 (Fig. 3a) contains several oli-

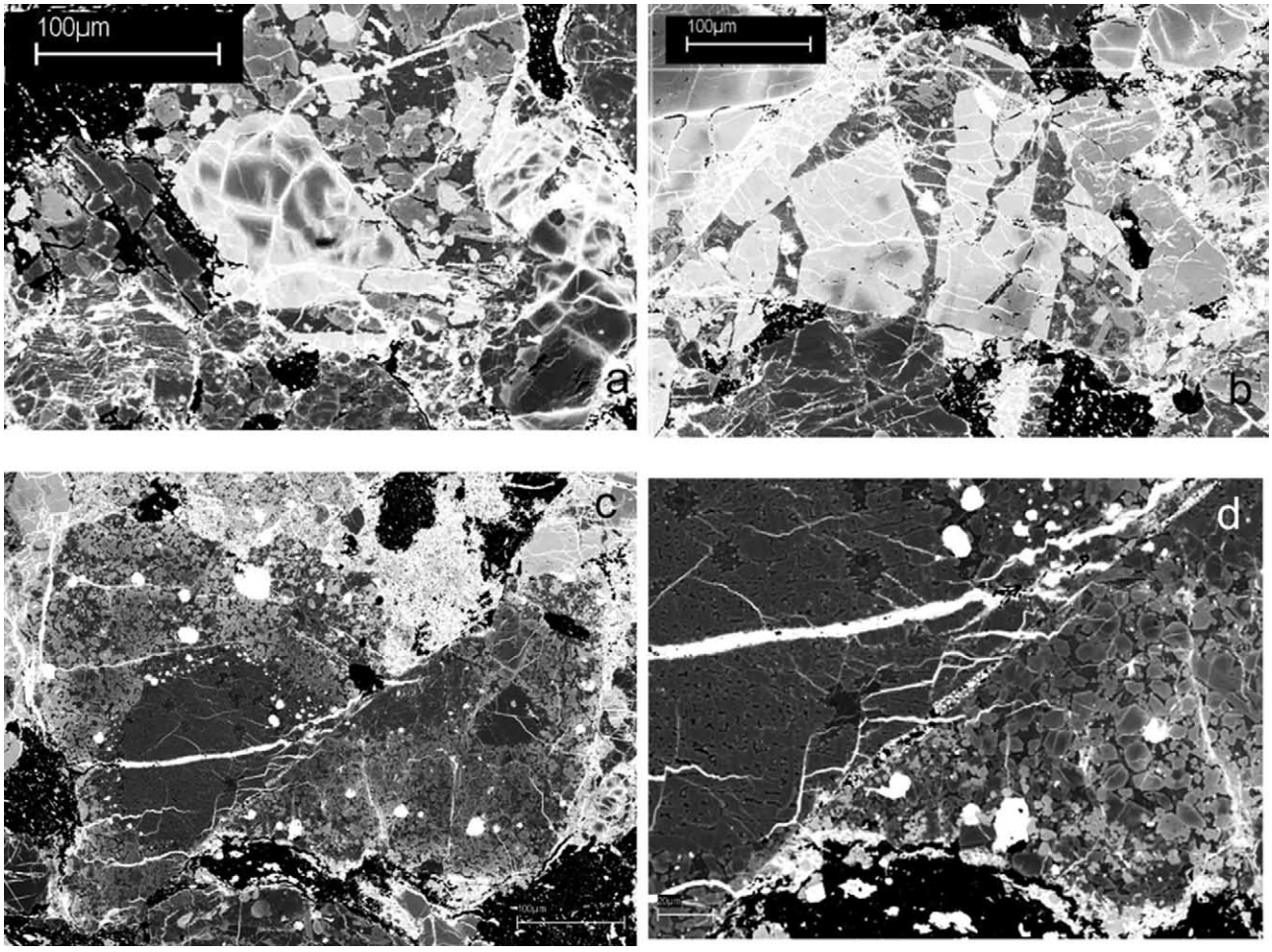

Fig. 6. Ferroan olivine in chondrules. (a) PO chondrule fragment C4 consists of low-FeO olivine cores (dark gray) surrounded by abundant ferroan olivine (light gray). Ferroan olivine also flanks most of the fractures (white). (b) Wedge-shaped PO chondrule fragment D3 containing large phenocrysts consisting of small residual low-FeO olivine cores (dark gray) surrounded by abundant ferroan olivine (light gray). (c) Compound chondrule G7 consisting of a recrystallized RP core surrounded by a PO spherical shell containing many small euhedral olivine grains with low-FeO cores surrounded by thin rims of ferroan olivine. The chondrule is bisected by a prominent fault. Scale bar at lower right is 100 μm in length. (d) Higher-magnification view of the fault transecting compound chondrule G7. The fault varies in width from 1.8 to 4.5 μm and has a displacement of ~180 μm. Also visible are the low-FeO cores and surrounding ferroan rims of the small euhedral olivine grains.

vine grains within the rim that consist of 3–6-μm-wide low-FeO cores (Fa1.2) surrounded by 1–2-μm-thick rinds of ferroan olivine (Fa21-25). Some of the olivine bars in the chondrule have moderately low-FeO cores rimmed by ferroan olivine. Some small, relatively equant bars consist completely of ferroan olivine; this is also the case for elongated olivine bars that have a half-width of 1–2 μm.

3.1.2.8. Faults. Several faults with a maximum length of ~1.2 mm and a maximum displacement of ~200 μm occur in PV1 (Figs. 6c,d, 7). The faults are oriented in different directions. One fault cuts across (and thus postdates) the fractures in chondrule F6, but another fault is transected by (and thus predates) the fractures in compound chondrule G7 (Fig. 6c). The fault that cuts across G7 has a wedge-shaped cross-section and varies in thickness from 1.8 to 4.5 μm (Fig. 6d). One ≥6-mm-long fault through the Plainview host transects the entire PV1 clast, dividing it into two unequal segments (~20 and ~80 vol%) (fig. 1a of Scott et al., 1981b; fig. 10 of Rubin, 1982). This particular fault is subparallel to two prominent metal veins that penetrate the clast from the Plainview host.

3.1.2.9. Carbon-rich patches. The abundant carbon in PV1 occurs mainly within irregularly shaped 30–400-μm-size opaque patches (Fig. 1b). Previous TEM studies showed the presence of poorly graphitized or turbostratic C associated with amorphous carbon (Brearley et al., 1987). Small (2–5 × 50–80 nm) carbon crystallites are present, but well-crystallized graphite is not (Brearley et al., 1987; Brearley, 1990). Approximately 10 wt% Fe is present within the C (Scott et al., 1981a,b), but the Fe does not occur as a distinct crystalline phase (Brearley et al., 1987).

There is no evidence of silicate reduction at the interfaces between the C-rich patches and adjacent silicate. Even small

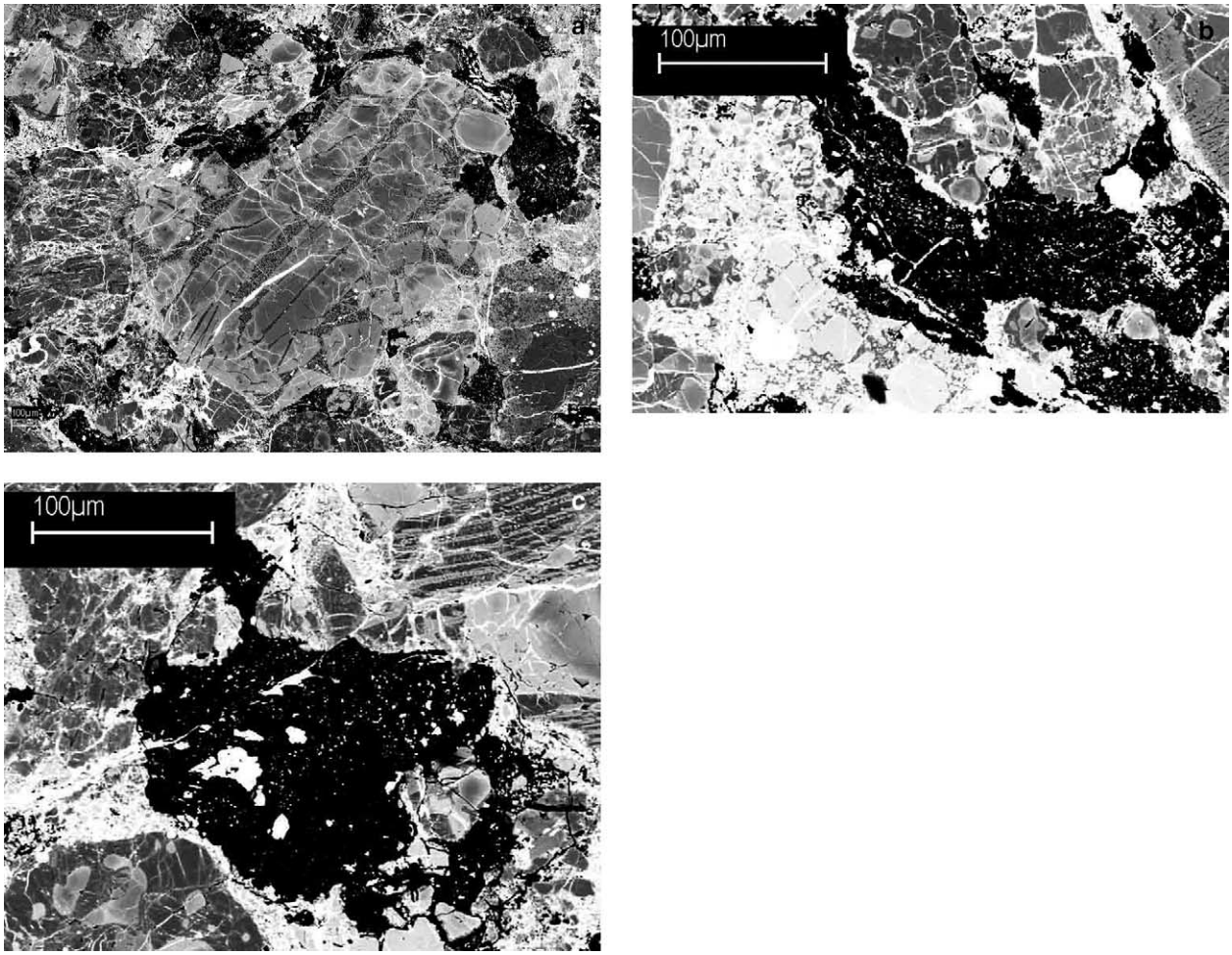

Fig. 7. Faults in chondrules. (a) Coarse-grained PO chondrule fragment F6 transected by a fault oriented NW-SE. The displacement on the fault is ~50 μm. At the top center is a 80 × 440-μm-size C-rich aggregate containing a 30-μm-long goethite vein bent at an angle of ~110° along the trajectory of a fault. (b) Aggregate I4 contains a 170-μm-long curvilinear vein of troilite along the trace of a fault. (c) Aggregate K2 contains a 110-μm-long taenite vein flanked by a 5-μm-thick mantle of goethite along the trace of a fault.

(3–10 μm) olivine grains completely embedded within the C show no such evidence. (If such reduction had occurred, portions of silicate grains adjacent to the C patches would show compositional gradients similar to those observed adjacent to graphite veins in ureilites, e.g., Berkley et al., 1976.) One might also expect "dusty olivine" (consisting of small blebs of Ni-poor metallic Fe) of the sort present in chondrules from type 3 chondrites (e.g., fig. 5b of Jones, 1996) to occur in PV1, but no such structures are present.

In several places (e.g., F6, I4, K2), the BSE images show bright-shaded veins within the C-rich material that trace the faults. In F6, a 1.8-μm-thick, 30-μm-long goethite vein within an 80 × 440-μm-size C-rich patch is bent at an angle of ~110° along the trajectory of a fault (Fig. 7a). In I4, a 1–2-μm-thick, 170-μm-long curvilinear vein of troilite lies along the trace of a fault within a 55 × 210-μm-size C-rich patch (Fig. 7b). In K2, a 110-μm-long, 1.4-μm-thick taenite vein flanked in places by a 5-μm-thick mantle of goethite lies along the trace of a fault within a 140 × 220-μm-size C-rich patch (Fig. 7c).

3.2. Bulk Chemical Composition

The concentrations of 25 elements in PV1, determined by INAA, are listed in Table 1. The Mg-normalized abundance ratios of these elements in PV1 relative to mean H-group chondrites are shown in Figure 8.

Refractory lithophile elements are all within 17% of H chondrites; they range from 0.86×H for Sm to 1.17×H for Ca. The mean refractory-lithophile-element abundance ratio for 10 elements (Al, Sc, Ca, REE) is 1.00 ± 0.09×H.

PV1 is depleted in the moderately volatile lithophile elements Na (0.75×H) and K (0.70×H).

Iridium, the only refractory siderophile element that was analyzed, is at 1.2×H. Common siderophile elements are all appreciably depleted: Ni (0.70×H), Co (0.43×H), Fe (0.67×H). In contrast, the volatile siderophile elements are relatively unfractionated: Au (1.05×H), As (0.93×H), Ga (1.10×H). Chalcophile Se (1.28×H) and Zn (1.38×H) abundances are moderately high in the PV1 clast.

Table 1. Concentrations of 25 elements determined by INAA in a 5.46-mg chip of Plainview clast PV1[a].

	C	Na	Mg	Al	K	Ca	Sc	V	Cr	Mn	Fe	Co	Ni	Zn	Ga	As	Se	La	Sm	Eu	Tb	Ho	Yb	Lu	Ir	Au
Clast PV1	130	5.65	172	13.0	665	17.6	9.27	85.5	4.38	3.10	219	435	13.9	76	7.7	2.41	12.6	350	200	97	67	80	262	38	1160	277
H chondrites	1.1	6.26	142	11.4	782	12.4	7.88	73.3	3.67	2.32	271	831	16.3	45.5	5.78	2.13	8.1	303	191	74	53	73	208	31.9	791	218

[a] Concentrations are in μg/g except: Na, Mg, Al, Ca, Cr, Mn, Fe, Ni in mg/g; REE, Ir, Au in ng/g. Also given is the C concentration (in mg/g) of PV1 estimated by Scott et al. (1981a, b). H-chondrite data from Kallemeyn et al. (1989) except for C, Tb and Ho (from Wasson and Kallemeyn, 1988).

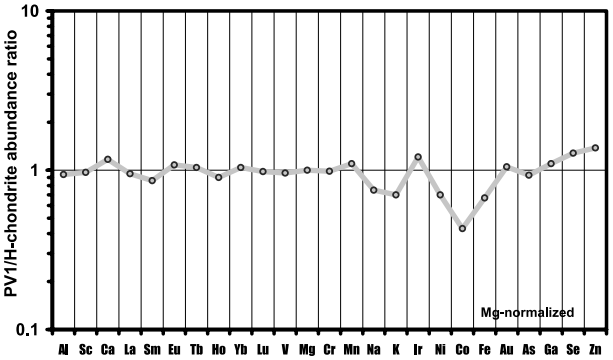

Fig. 8. H-chondrite- and Mg-normalized abundance ratios of 25 elements measured in clast PV1 by INAA. Lithophile elements are plotted at the left and siderophile and chalcophile elements at the right. In each group, elements are arranged from left to right in order of decreasing nebular condensation temperature. The mean refractory lithophile abundance ratio for 10 elements (Al–Lu) is 1.00×H-chondrites. The semirefractory and common lithophiles are also unfractionated; moderately volatile Na and K are moderately depleted. The siderophile element pattern is more complex: refractory Ir is moderately enriched, the common siderophiles (Ni, Co, Fe) are depleted, and the volatile siderophiles (Au, As, Ga) are essentially unfractionated. The two chalcophiles (Se, Zn) are moderately enriched.

4. DISCUSSION

4.1. H3 Chondrite Precursor

4.1.1. H-group chondrite precursor

There are several characteristics of clast PV1 that indicate that it formed from H-group chondrite material. Chondrules in PV1 have a mean apparent diameter of 310 ± 120 μm, essentially identical to that of mean H3-chondrite chondrules (~300 μm; Rubin, 2000). (For comparison, L and LL chondrites have mean chondrule diameters of ~500 and ~570 μm, respectively; Rubin, 2000; Nelson and Rubin, 2002.) The PV1 INAA data show a mean Mg-normalized refractory lithophile abundance ratio (Al, Sc, Ca, La, Sm, Eu, Tb, Ho, Yb, Lu) relative to H chondrites of 1.00 ± 0.09, i.e., indistinguishable from that of mean H chondrites. The O-isotopic composition of PV1 ($\delta^{18}O$ = 3.35‰; $\delta^{17}O$ = 2.40‰; Scott et al., 1988) yields a $\Delta^{17}O$ value of 0.66‰, within one standard deviation of that of mean H4-6 chondrites ($\Delta^{17}O$ = 0.73 ± 0.09‰; n = 22; Clayton et al., 1991) and very similar to the mean of the two H3 falls (Sharps and Dhajala) analyzed by Clayton et al.: 0.68 ± 0.04‰.

Because most material in lunar breccias is derived from local bedrock (McKay et al., 1991), it seems more likely that the four known C-rich chondritic clasts (all of which occur in H-chondrite regolith breccias; Scott et al., 1981b) were derived from the H-chondrite asteroid than from an external source. In contrast, CM2 chondrite clasts occur not only in H-chondrite regolith breccias (e.g., Plainview, Abbott, Tysnes Island, Ipiranga; Fodor and Keil, 1976; Fodor et al., 1976; Keil and Fodor, 1980; Rubin, 1982), but also in CV3 Leoville (Keil et al., 1969), several howardites (e.g., Kapoeta, Bholghati, G'Day, Jodzie, LEW 85441, LEW 87015; Wilkening, 1973; Buchanan et al., 1993; Zolensky et al., 1996) and the LEW 87295 polymict eucrite (Zolensky et al., 1996). The wide distribution

of CM2 clasts in regolith and near-surface fragmental breccias from different asteroids indicates that they were derived from an external source.

4.1.2. Type 3 chondrite precursor

It is probable that PV1 started off as a type 3 chondrite because of the presence of glass in some BO, PO and POP chondrules (e.g., Fig. 3a) and the juxtaposition of low-FeO and high-FeO chondrules (Fig. 1b). Although the overall olivine and low-Ca pyroxene compositional distributions (Fig. 2; fig. 4 of Scott et al., 1981b) were affected by subsequent hydrothermal alteration and partial metamorphic equilibration (see below), the composition of olivine cores in PV1 (which reflect nebular compositions more closely) has a minimum range of Fa1-19.

Normal primitive type 3 OC contain ~10–15 vol% fine-grained, FeO-rich silicate matrix material (table 4 of Huss et al., 1981). In addition, ~7% of their chondrules are RP and cryptocrystalline textural types (Nelson and Rubin, 2002). Although the apparent absence of matrix material and dearth of RP and cryptocrystalline chondrules in PV1 is nominally inconsistent with the hypothesis that this clast started off as a normal H3 chondrite, altered forms of these materials appear to be present. We observed materials that we infer to be recrystallized clumps of matrix material (i.e., I5; Fig. 5c), and thermally altered fragments of RP and cryptocrystalline chondrules (i.e., (i.e., Figs. 5a,b). This is consistent with the hypothesis that PV1 silicates were normal type 3 OC material before impact heating (see below).

We also note that the C-isotopic composition of PV1 ($\delta^{13}C_{PDB} = -21‰$; Scott et al., 1988) is marginally within the range of type 3 OC falls (−20.6 to −27.5‰; mean $\delta^{13}C_{PDB} = -23.6 \pm 2.0‰$; $n = 10$; Grady et al., 1982) but outside the range of type 4–6 OC (typically −25 to −30‰; Grady et al., 1982). This is consistent with C in PV1 having the same general provenance as C in type 3 OC.

4.2. Impact Heating

If PV1 was initially a normal H3 chondrite, it would have had ~18 wt% metallic Fe-Ni and ~5.4 wt% troilite (Jarosewich, 1990). In contrast, modal analysis indicates that PV1 contains ~<6 vol% (i.e., ~<14 wt%) metallic Fe-Ni, and ~7 vol% (i.e., ~10 wt%) troilite (Scott et al., 1981b); these phases appear to be heterogeneously distributed (Fig. 1c). The modal abundances of metal and troilite in the clast were probably enhanced by the inclusion in the modal analysis of late-formed vein materials. These materials may have had a high troilite/metal ratio, possibly similar to that of a eutectic mixture (7.5:1). The clast thus lost a significant fraction of the original H3 metal; it must also have lost appreciable troilite. Moderate depletion of metallic Fe-Ni in PV1 is indicated by the Mg- and H-chondrite-normalized abundance ratios of the common siderophile elements Fe (0.67), Ni (0.70) and Co (0.43) in the bulk analysis (Table 1; Fig. 8). The possibility of significant loss of metal from PV1 due to terrestrial weathering can be discounted because the surrounding Plainview host is not depleted in metallic Fe-Ni (Fig. 1).

Loss of metal requires a high-temperature event wherein temperatures reached or exceeded the Fe-FeS eutectic (988°C; Kullerud, 1963) and where shear forces separated metal-sulfide liquid from silicate solids. This event is likely to have been impact heating on the parent body with associated separation of a metal-sulfide melt. Many impact-melt-rock clasts in chondritic meteorites are highly depleted in metallic Fe-Ni and troilite (e.g., Fodor et al., 1972; Fodor and Keil, 1976; Wilkening, 1978). The somewhat heterogeneous distribution of metal and sulfide in PV1 suggests that some portions of the clast may not have reached the Fe-FeS eutectic. Quenching may have preserved the glass in some of the chondrules (particularly in those regions that may have experienced somewhat lower maximum temperatures).

The siderophile/chalcophile elemental abundance pattern in PV1 is complex (Fig. 8). There are moderate depletions of common siderophiles, relatively unfractionated abundances of volatile siderophiles, a moderate enrichment in refractory Ir, and (consistent with the moderately high modal abundance of troilite) moderate enrichment in the chalcophiles Se and Zn. This complex pattern may partly reflect sampling variations, loss of some metal and sulfide during the impact event, and, probably, late-stage introduction of metal and sulfide from outside the clast.

There is additional evidence for a high-temperature event. Our BSE images of PV1 reveal that most interfaces between adjacent chondrules are fused together (Fig. 4), rendering the clast somewhat analogous to a conglomerate of compound-chondrule clusters wherein each cluster consists of >20 individual chondrules. Such chondrule fusion requires temperatures that exceeded the solidus temperature for H chondrites, which is <1120°C (Jurewicz et al., 1995) and probably closer to 1100°C. Melting and partial loss of feldspathic components (including chondrule glass), possibly combined with loss of a volatile-rich vapor, is consistent with the depletion of moderately volatile lithophile elements in PV1: the Mg- and H-chondrite-normalized abundance ratios of Na and K are 0.75 and 0.70, respectively (Table 1; Fig. 8).

PV1 also contains several objects (e.g., I5; Fig. 5c) that appear to be recrystallized clumps of fine-grained silicate matrix material. We suggest that the apparent absence in PV1 of fine-grained silicate-rich matrix material is a consequence of the impact heating and recrystallization of this material.

The recrystallized RP and cryptocrystalline chondrules (e.g., objects E6, D2) in PV1 are also consistent with shock heating of the clast.

By analogy with porous, melt-bearing fragmental breccias found in impact-crater ejecta deposits (Stöffler et al., 1980), it seems plausible that, at this stage, the PV1 precursor lithology had a high porosity. The voids may have been the sites where C-rich material was later incorporated (see below).

It has been suggested that PV1 could be a heterogeneous mixture of materials with different heating histories. However, the occurrence of clusters of fused chondrules throughout the clast attests to fairly uniform heating.

In an attempt to circumvent this difficulty, Brearley suggested that the melded chondrule boundaries were not caused by fusion at high temperatures, but rather may have resulted from pressure solution as is the case for ooids (a.k.a. ooliths—millimeter-size, spheroidal inorganic precipitates) in some terrestrial sedimentary rocks (fig. 2 of Skinner, 1989). However,

some of the ooids shown by Skinner appear to be fragmented, a likely occurrence in the shallow, wave-agitated water where ooids are produced. Some of the apparently conjoined ooids could be juxtaposed fragments that were jostled into place rather than melded together by pressure solution. In any case, low-temperature pressure solution is less likely to affect mafic minerals in chondrules than calcium carbonate in ooids. Furthermore, the melded chondrules in PV1 differ significantly from melded ooids in being recrystallized in regions away from boundary surfaces.

4.3. Hydrothermal Alteration

The typical small euhedral olivine grains within compound chondrule G7 in PV1 consist of 3–5-μm-size low-FeO cores rimmed by ferroan olivine (Fig. 6d). Narrow fractures in many of these grains are also filled with ferroan olivine. The grains closely resemble the altered olivine grains in amoeboid olivine inclusions (AOIs) in CO3.2–3.5 chondrites wherein ferroan olivine conforms to the shapes of preexisting cracks and to the outlines of grain boundaries (Chizmadia et al., 2002). Numerous coarser olivine grains within porphyritic chondrules throughout PV1 (e.g., Fig. 6) are analogous to these small grains: they also consist of low-FeO cores surrounded by thick patches of ferroan olivine.

The ferroan olivine patches in PV1 were probably caused by hydrothermal alteration at low water/rock ratios. The ferroan olivine rims are more fayalitic than the average for equilibrated H chondrites (Fa17.3–20.2; Rubin, 1990); thus, some form of alteration process must be responsible for their formation. This process is not likely to be aqueous alteration sensu stricto because of the elevated temperatures, the apparent absence of hydrous phases in the clast, and the preservation of chondrule glass. It seems probable that some metallic Fe was oxidized and that the resultant FeO, combined with SiO_2 derived from fine-grained phases, was transported by a fluid along grain boundaries and through preexisting fractures in the low-FeO olivine grains; it was at these sites that fayalitic olivine precipitated.

Temperatures were high enough in PV1 to allow minor volume diffusion in the olivine: Fe^{+2} from the newly precipitated fayalitic olivine exchanged partially with Mg^{+2} from adjacent low-FeO olivine to form diffusive haloes of ferroan olivine around the low-FeO olivine cores. The effective distance for volume diffusion in PV1 olivine during this event is ~1–2 μm as indicated by the thickness of the ferroan olivine rinds around low-FeO cores in the rim of BO chondrule B4 (Fig. 3a).

There is a paucity of olivines of composition Fa0-3 in H/L3.6 Tieschitz (fig. 1 of Dodd et al., 1967) presumably caused by partial equilibration of olivine during metamorphism. Similarly, the olivine compositional distribution in PV1 shows a paucity of Fa0-2 olivine grains (Fig. 2a), presumably also due to partial equilibration. In contrast, histograms of olivine distributions in more primitive type 3 OC (e.g., LL3.0 Semarkona) are bimodal with a sharp peak at low-FeO compositions (e.g., fig. 1 of Takagi et al., 2004).

The heat responsible for hydrothermal alteration and diffusion may be residual shock heat that resulted from impact heating and burial of the clast.

4.4. Fracturing

The numerous 20–160-μm-long fractures that transect every chondrule in PV1 (e.g., Fig. 3b) were caused by crushing, presumably also associated with an impact event. Most fracturing postdated impact heating; if fracturing had preceded impact heating, it seems likely that the fractures in recrystallized silicate matrix object I5 in PV1 would have been largely obliterated.

4.5. Potential Sources of Carbon

We suggest two potential source regions for the C-rich material in the chondritic clasts: the solar nebula and the H-chondrite parent asteroid. We have discussed the evidence indicating that the PV1 precursor was initially a normal H3 chondrite. Because type 3 OC contain ~<1 wt% C (Jarosewich, 1990), we think it unlikely that the C-rich clasts obtained their abundant C during nebular agglomeration. We therefore conclude that the clasts acquired their C on the H-chondrite asteroid.

Two mechanisms that could potentially account for C enrichment on the parent body are (1) outgassing of CO from the asteroid interior and (2) introduction of C from a C-rich projectile.

4.5.1. Outgassing

It is conceivable that the C was derived by outgassing of CO from metamorphosed (H4-6) rocks in the asteroid interior followed by dissociation of the CO to form C within permeable materials near the asteroid surface (Sugiura et al., 1986). One possible reaction is:

$$Fe(s) + CO(g) + MgSiO_3(s) \rightarrow FeMgSiO_4(s) + C(s) \quad (1)$$

In this reaction, oxidation of 10 wt% Fe would yield ~2 wt% C. This value is higher than that in type 3 OC (which typically contain ~<1 wt% C), but much lower than that in PV1 (13 wt%). Although PV1 is depleted in metallic Fe relative to normal H-group chondrites by ≥4 wt%, a portion of this depletion is attributable to loss of a metal-rich liquid during an impact event. Thus, the moderately low concentration of Fe in PV1 cannot be attributed solely to oxidation of Fe as shown in Eqn. 1. In addition, thermodynamic data indicate that at T <1100 K and pCO <1 atm, the reverse reaction would spontaneously occur.

4.5.2. C-rich projectile

Another possibility is that the C was delivered as carbonaceous matter derived from a C-rich projectile. The most C-rich planetesimal-size projectiles are comets. Jessberger et al. (1988) reported that the dust + ice fraction of Comet Halley contains ~19 wt% C, although some estimates of the C contents of comets are appreciably lower (e.g., ~8 wt%; Delsemme, 1982). Carbon occurs in comets in a wide variety of phases including simple, volatile species (e.g., CO, CO_2), complex, multiatomic species (e.g., $HCOOCH_3$, $HOCH_2CH_2OH$—ethylene glycol), organic (CHON) grains, and organic refractory coatings on silicate grains (e.g., Mumma et al., 1993; Rahe

et al., 1995; Greenberg, 1998). By analogy with CI and CM chondrites, complex hydrocarbons and kerogen (Cronin et al., 1988) that cannot be detected by remote studies are probably present as well. The high-molecular-weight compounds tend to be relatively refractory and would likely be the most important precursors of the carbon in PV1.

It seems possible that the hypothetical cometary projectile served as the source of the fluid responsible for the hydrothermal alteration of PV1, but the silicate portion of the comet is not a recognizable component of the clast.

It is not unreasonable that a cometary impact could have affected the chondritic clasts. A small fraction of Jupiter-family comets (JFCs) evolve into near-Earth objects (Levison and Duncan, 1997) and could impact main-belt asteroids at relatively low velocities of ~5 km s^{-1} (similar to those of average asteroid/asteroid collisions) (Campins and Swindle, 1998). Recent studies estimate that ~1% of the projectiles impacting asteroids today are JFCs (Wetherill, 1978; Near-Earth Object Science Definition Team, 2003).

It is conceivable that the carbon in the C-rich chondritic clasts was derived from liquid hydrocarbons that flowed into voids in the clast. Such liquids could have been subsequently broken down into carbonaceous matter with high C/H ratios by dehydrogenation processes perhaps resulting from heat generated by the same impact event(s) that fractured and faulted the clast. The $\delta^{13}C_{PDB}$ composition of PV1 (−21‰; Scott et al., 1988) is within the wide range reported for comets (−11‰ to −43‰; Wyckoff et al., 2000) as well as that of type 3 OC falls (−20.6 to −27.5‰; Grady et al., 1982).

4.6. Inferred History of PV1

A volume of H3 material, residing in the near-surface region of the H-chondrite asteroid, was impact heated. The nature of the projectile responsible for this event is unknown. Temperatures in the clast reached ~1100°C and chondrules throughout PV1 fused together into clusters. Fine-grained ferroan silicate matrix material was recrystallized, and, in some regions of the clast, fine-grained RP and cryptocrystalline chondrule textural types were similarly affected. Some metal and sulfide melted and separated from solid silicate, and the rock was left with numerous impact-induced voids.

At a later time, a C-rich projectile accreted to the parent asteroid; the PV1 precursor was fractured during this event. Carbon from the (presumably cometary) projectile filled the voids; the carbon may have been transported as a fluid that later broke down into elemental C. The impact of this projectile probably caused moderate heating of the clast. Annealing at 300 to 450°C caused the graphitizable organic C in PV1 to pyrolyze and dehydrogenate, thereby transforming it into poorly graphitized C (Brearley, 1990). Additional impact events caused fracturing in the clast and surrounding materials in the Plainview regolith.

While the clast remained at elevated temperatures, hydrothermal alteration at low water/rock ratios caused partial equilibration of PV1, resulting in the paucity of forsterite grains in the olivine compositional distribution. This process also caused oxidation of some metallic Fe; FeO combined with SiO_2 derived from fine-grained phases and was transported by a fluid through fractures and along grain boundaries where it precipitated as fayalite. Ferroan olivine haloes formed around the low-FeO olivine cores.

Before PV1 was incorporated into the Plainview host, the host was thermally metamorphosed to petrologic type 5, reaching temperatures of ~500 to 600°C. If the Plainview host had been metamorphosed after the C-rich PV1 clast was incorporated, chondrule glass in PV1 would have recrystallized.

A subsequent impact event (or series of events) dislodged the PV1 clast from its formation region and deposited it into its final location in the H-chondrite regolith. Other C-rich chondritic clasts were deposited elsewhere in the regolith. This is indicated by the different cosmic-ray exposure ages of the regolith breccias that contain these clasts (Plainview, 6.0 Ma; Dimmitt, 6.0 Ma; Weston, 35.5 Ma; Graf and Marti, 1995), demonstrating that the breccias were derived from different locations on the parent asteroid. After being incorporated into its final regolithic location, one or more additional impact event(s) caused extensive faulting in the Plainview host and PV1 clast.

Some of the C-rich aggregates that occur in the relatively C-rich type 3 OC (e.g., Sharps, ALHA77011) may have been derived from disrupted C-rich chondritic clasts similar to PV1 (Scott et al., 1981a). However, the abundant metallic Fe-Ni and minor chromite in most C-rich aggregates (Scott et al., 1988; Brearley, 1990) indicate different sources or more complex histories.

Acknowledgments—We thank the Institute of Meteoritics at the University of New Mexico for the chip of clast PV1 and the loan of Plainview thin section UNM 273. We gratefully acknowledge informative discussions with E. R. D. Scott and A. J. Brearley. The article benefited from thorough reviews by E. R. D. Scott, M. E. Zolensky, and particularly A. J. Brearley. This work was supported in part by NASA grants NAG5-12967 (A. E. Rubin) and NAG5-12887 (J. T. Wasson). J. M. Trigo-Rodriguez thanks the Spanish Secretary of Education and Universities for a postdoctoral grant.

Associate editor: M. Grady

REFERENCES

Berkley J. L., Brown H. G., Keil K., Carter N. L., Mercier J-C. C., and Huss G. (1976) The Kenna ureilite: An ultramafic rock with evidence for igneous, metamorphic and shock origin. *Geochim. Cosmochim. Acta* **40,** 1429–1437.

Bischoff A., Rubin A. E., Keil K., and Stöffler D. (1983) Lithification of gas-rich chondrite regolith breccias by grain boundary and localized shock melting. *Earth Planet. Sci. Lett.* **66,** 1–10.

Brearley A. J. (1990) Carbon-rich aggregates in type 3 ordinary chondrites: Characterization, origins and thermal history. *Geochim. Cosmochim. Acta* **54,** 831–850.

Brearley A. J., Scott E. R. D., and Keil K. (1987) Carbon-rich aggregates in ordinary chondrites: Transmission electron microscopy observation of Sharps (H3) and Plainview (H regolith breccia) (abstract). *Meteoritics* **22,** 33819.

Buchanan P. C., Zolensky M. E., and Reid A. M. (1993) Carbonaceous chondrite clasts in the howardites Bholghati and EET 87513. *Meteoritics* **28,** 659–669.

Campins H. and Swindle T. D. (1998) Expected characteristics of cometary meteorites. *Meteorit. Planet. Sci.* **33,** 1201–1211.

Chizmadia L. J., Rubin A. E., and Wasson J. T. (2002) Mineralogy and petrology of amoeboid olivine inclusions in CO3 chondrites: Relationship to parent-body aqueous alteration. *Meteorit. Planet. Sci.* **37,** 1781–1796.

Clayton R. N., Mayeda T. K., Goswami J. N., and Olsen E. J. (1991) Oxygen isotope studies of ordinary chondrites. *Geochim. Cosmochim. Acta* **55,** 2317–2337.

Cronin J. R., Pizzarello S. and Creikshank D. P. (1988) Organic matter in carbonaceous chondrites, planetary satellites, asteroids and com-

ets. In *Meteorites and the Early Solar System* (eds. J. F. and Kerridge M. S. Matthews), pp. 819–857. University of Arizona Press, Tucson.

Delsemme A. H. (1982) Chemical composition of cometary nuclei. In *Comets* (eds. L. L. and Wilkening M. S. Matthews), pp. 85–130. University of Arizona Press, Tucson.

Dodd R. T., Van Schmus W. R., and Koffman D. M. (1967) A survey of the unequilibrated ordinary chondrites. *Geochim. Cosmochim. Acta* **31,** 921–951.

Fodor R. V., Keil K., and Jarosewich E. (1972) The Oro Grande, New Mexico, chondrite and its lithic inclusion. *Meteoritics* **7,** 495–507.

Fodor R. V. and Keil K. (1976) Carbonaceous and noncarbonaceous lithic fragments in the Plainview, Texas chondrite: Origin and history. *Geochim. Cosmochim. Acta* **40,** 177–189.

Fodor R. V., Keil K., Wilkening L. L., Bogard D. D., and Gibson E. K. (1976) Origin and history of a meteorite parent-body regolith breccia: Carbonaceous lithic fragments in the Abbott, New Mexico, chondrite. *Special Pub. New Mexico Geol. Soc.* **6,** 206–218.

Graf T. and Marti K. (1995) Collisional history of H chondrites. *J. Geophys. Res.* **100,** 21247–21263.

Grady M. M. (2000) *Catalogue of Meteorites.* Cambridge University Press.

Grady M. M., Swart P. K., and Pillinger C. T. (1982) The variable carbon isotopic composition of type 3 ordinary chondrites. *Proc. Lunar Planet. Sci. Conf.* **13,** A289–A296.

Greenberg J. M. (1998) Making a comet nucleus. *Astron. Astrophys.* **330,** 375–380.

Huss G. R., Keil K., and Taylor G. J. (1981) The matrices of unequilibrated ordinary chondrites: Implications for the origin and history of chondrites. *Geochim. Cosmochim. Acta* **45,** 33–51.

Jarosewich E. (1990) Chemical analyses of meteorites: A compilation of stony and iron meteorite analyses. *Meteoritics* **25,** 323–337.

Jessberger E. K., Christoforidis A., and Kissel J. (1988) Aspects of the major element composition of Halley's dust. *Nature* **332,** 691–695.

Jones R. H. (1996) Relict grains in chondrules: Evidence for chondrule recycling. In *Chondrules and the Protoplanetary Disk* (eds. R. H. Hewins, R. H., and Jones E. R. D. Scott), pp. 163–172. Cambridge University Press. USA.

Jurewicz A. J. G., Mittlefehldt D. W., and Jones J. H. (1995) Experimental partial melting of the St. Severin (LL) and Lost City (H) chondrites. *Geochim. Cosmochim. Acta* **59,** 391–408.

Kallemeyn G. W., Rubin A. E., Wang D., and Wasson J. T. (1989) Ordinary chondrites: Bulk compositions, classification, lithophile-element fractionations and composition-petrographic type relationships. *Geochim. Cosmochim. Acta* **53,** 2747–2767.

Keil K., Huss G. I. and Wiik H. B. (1969) The Leoville, Kansas, meteorite: A polymict breccia of carbonaceous chondrites and achondrite (abstract). In *Meteorite Research* (ed. P. M. Millman), p. 217. D. Reidel, Dordrecht.

Keil K. and Fodor R. V. (1980) Origin and history of the polymict-brecciated Tysnes Island chondrite and its carbonaceous and non-carbonaceous lithic fragments. *Chem. Erde* **39,** 1–26.

Keil K., Fodor R. V., Starzyk P. M., Schmitt R. A., Bogard D. D., and Husain L. (1980) A 3.6-b.y.-old impact-melt rock fragment in the Plainview chondrite: Implications for the age of the H-group chondrite parent body regolith formation. *Earth Planet. Sci. Lett.* **51,** 235–247.

Kullerud G. (1963) The Fe-Ni-S system. *Carnegie Inst. Wash. Yr. Bk.* **62,** 175–189.

Levison H. F. and Duncan M. J. (1997) From the Kuiper Belt to Jupiter-family comets: The spatial distributions of ecliptic comets. *Icarus* **127,** 13–32.

McKay D. S., Heiken G., Basu A., Blanford G., Simon S., Reedy R., French B. M. and Papike J. (1991) The lunar regolith. In: *Lunar Sourcebook: A User's Guide to the Moon* (eds. G. H. Heiken, D. T. and Vaniman B. M. French), pp. 285–356. Cambridge University Press. USA.

McKinley S., Scott E. R. D., Taylor G. J., and Keil K. (1981) A unique type 3 chondrite containing graphite-magnetite aggregates—Allan Hills A77011. *Proc. Lunar Planet. Sci.* **12B**, 1039–1048.

McSween H. Y. and Richardson S. M. (1977) The composition of carbonaceous chondrite matrix. *Geochim. Cosmochim. Acta* **41,** 1145–1161.

Mostefaoui S., Perron C., Zinner E., and Sagon G. (2000) Metal-associated carbon in primitive chondrites: Structure, isotopic composition and origin. *Geochim. Cosmochim. Acta* **64,** 1945–1964.

Mumma M. J., Stern S. A. and Weisman P. R. (1993) Comets and the origin of the solar system. In *Protostars and Planets III* (eds. E. H. and Levy J. L. Lunine), pp. 1177–1252. University of Arizona Press, Tucson.

Near-Earth Object Science Definition Team (2003) *Study to Determine the Feasibility of Extending the Search for Near-Earth Objects to Smaller Limiting Diameters*. NASA.

Nelson V. E. and Rubin A. E. (2002) Size-frequency distributions of chondrules and chondrule fragments in LL3 chondrites: Implications for parent-body fragmentation of chondrules. *Meteorit. Planet. Sci.* **37,** 1361–1376.

Rahe J., Vanysek V. and Weissman P. R. (1995) Properties of cometary nuclei. In *Hazards Due to Comets and Asteroids* (ed. T. Gehrels), pp. 597–634. University of Arizona Press, Tucson.

Rubin A. E. (1982) Petrology and origin of brecciated chondritic meteorites. Ph.D. thesis. University of New Mexico, Albuquerque.

Rubin A. E. (1990) Kamacite and olivine in ordinary chondrites: Intergroup and intragroup relationships. *Geochim. Cosmochim. Acta* **54,** 1217–1232.

Rubin A. E. (2000) Petrologic, geochemical and experimental constraints on models of chondrule formation. *Earth Sci. Rev.* **50,** 3–27.

Schultz L. and Kruse H. (1989) Helium, neon and argon in meteorites—A data compilation. *Meteoritics* **24,** 155–172.

Scott E. R. D., Taylor G. J., Rubin A. E., Okada A., and Keil K. (1981a) Graphite-magnetite aggregates in ordinary chondritic meteorites. *Nature* **291,** 544–546.

Scott E. R. D., Rubin A. E., Taylor G. J., and Keil K. (1981b) New kind of type 3 chondrite with a graphite-magnetite matrix. *Earth Planet. Sci. Lett.* **56,** 19–31.

Scott E. R. D., Brearley A. J., Keil K., Grady M. M., Pillinger C. T., Clayton R. N., Mayeda T. K., Wieler R., and Signer P. (1988) Nature and origin of C-rich ordinary chondrites and chondritic clasts. *Proc. Lunar Planet. Sci. Conf.* **18,** 513–523.

Skinner W. R. (1989) Compaction and lithification of chondrites (abstract). *Lunar Planet. Sci.* **20,** 1020–1021.

Stöffler D., Knöll H.-D., Marvin U. B., Simonds C. H. and Warren P. H. (1980) Recommended classification and nomenclature of lunar highland rocks—A committee report. In *Proc. Conf. Lunar Highlands Crust* (ed. R. B. and Merrill J. J. Papike), pp. 51–70. Pergamon. USA.

Stöffler D., Keil K. and Scott E. R. D. (1991) Shock metamorphism of ordinary chondrites. *Geochim. Cosmochim. Acta* **55,** 3845–3867.

Sugiura N., Arkani-Hamed J., and Strangeway D. W. (1986) Possible transport of carbon in meteorite parent bodies. *Earth Planet. Sci. Lett.* **78,** 148–156.

Takagi M., Huber H., Rubin A. E., and Wasson J. T. (2004) Distribution of FeO/(FeO + MgO) in Semarkona chondrules: Implications for chondrule formation and nebular evolution (abstract). *Meteorit. Planet. Sci.* 39:A103.

Wasson J. T. and Kallemeyn G. W. (1988) Compositions of chondrites. *Phil. Trans. R. Soc. Lond. A* **325,** 535–544.

Wasson J. T., Krot A. N., Lee M. S., and Rubin A. E. (1995) Compound chondrules. *Geochim. Cosmochim. Acta* **59,** 1847–1869.

Wetherill G. W. (1978) Dynamical evidence regarding the relationship between asteroids and meteorites. In *Asteroids: An Exploration Assessment,*pp. 17–35. Conf. Pub. 2053. NASA.

Wilkening L. L. (1973) Foreign inclusions in stony meteorites—I. Carbonaceous xenoliths in the Kapoeta howardite. *Geochim. Cosmochim. Acta* **37,** 1985–1989.

Wilkening L. L. (1978) Tysnes Island: An unusual clast composed of solidified, immiscible, Fe-FeS and silicate melt. *Meteoritics* **13,** 1–9.

Wyckoff S., Kleine M., Peterson B. A., Wehinger P. A., and Ziurys L. M. (2000) Carbon isotope abundances in comets. *Astrophys. J.* **535,** 991–999.

Zolensky M. E., Weisberg M. K., Buchanan P. C., and Mittlefehldt D. W. (1996) Mineralogy of carbonaceous chondrite clasts in HED achondrites and the moon. *Meteorit. Planet. Sci.* **31,** 518–537.